NEUROSCIENCE

MHC class I in dopaminergic neurons suppresses relapse to reward seeking

Gen Murakami,[1,2,3]* Mitsuhiro Edamura,[1] Tomonori Furukawa,[4] Hideya Kawasaki,[2] Isao Kosugi,[2] Atsuo Fukuda,[4] Toshihide Iwashita,[2] Daiichiro Nakahara[1,5]*

Major histocompatibility complex class I (MHCI) is an important immune protein that is expressed in various brain regions, with its deficiency leading to extensive synaptic transmission that results in learning and memory deficits. Although MHCI is highly expressed in dopaminergic neurons, its role in these neurons has not been examined. We show that MHCI expressed in dopaminergic neurons plays a key role in suppressing reward-seeking behavior. In wild-type mice, cocaine self-administration caused persistent reduction of MHCI specifically in dopaminergic neurons, which was accompanied by enhanced glutamatergic synaptic transmission and relapse to cocaine seeking. Functional MHCI knockout promoted this addictive phenotype for cocaine and a natural reward, namely, sucrose. In contrast, wild-type mice overexpressing a major MHCI gene (H2D) in dopaminergic neurons showed suppressed cocaine seeking. These results show that persistent cocaine-induced reduction of MHCI in dopaminergic neurons is necessary for relapse to cocaine seeking.

INTRODUCTION

Major histocompatibility complex class I (MHCI) is a cell surface protein that is responsible for antigen presentation to immune cells. Antigen peptides are transported into the endoplasmic reticulum via transporter associated with antigen processing (TAP). In mouse endoplasmic reticulum, antigens bind to the light chain [β-2 microglobulin (β2M)] and a heavy chain (for example, H2D or H2K) of MHCI. This complex is then transferred to the cell surface and recognized by appropriate T cells. Double-knockout (KO) mice of β2M and TAP are defective in stable assembly and intracellular transport of MHCI, which results in impaired surface expression of MHCI (*1*). Consequently, these double-KO mice are often used as functional MHCI KO mice. Although MHCI is expressed in nearly all nucleated cells, including neural cells, the brain has traditionally been considered an immune privileged region. However, MHCI plays an important role in synapse elimination in addition to its immune system role in mammalian brain (*2*). Recently, the neuron-specific role of MHCI has gained much attention, particularly in brain regions related to learning and memory, such as the hippocampus and cerebral cortex (*3*–*5*). In these brain regions, MHCI binds and signals via a key MHCI receptor, paired immunoglobulin-like receptor B (PirB), which is expressed in neuronal subsets throughout the brain, including glutamatergic neurons (*6*, *7*). PirB also functions as a β-amyloid receptor, and its activation leads to interaction with cofilin, an actin-severing protein that facilitates actin depolymerization, and results in altered synaptic plasticity and synaptic loss associated with Alzheimer's disease (*5*). Furthermore, in functional MHCI KO mice, elimination of long-term depression and enhancement of long-term potentiation leads to extensive synaptic transmission in the hippocampus and cerebral cortex (*8*, *9*), which ultimately results in learning and memory deficits (*10*). Although MHCI is highly expressed in the dopaminergic neuron-rich, ventral tegmental area (VTA), a region important for brain reward functions, the contribution of MHCI to this function has not previously been considered.

Addiction is a homeostatic disorder of brain reward function that is characterized by vulnerability to relapse of reward-seeking behavior even after long abstinence (*11*). Although drug addiction remains a serious public health problem worldwide, there are still no effective pharmacological drugs available. Hence, further understanding of the mechanisms underlying drug addiction is important for identifying novel factors that can be targeted for pharmacological treatment. In a previous study, we established a novel, drug self-administration system for mice, using an intrathecal microdialysis technique (*12*). Our method enabled daily 24-hour unlimited access to addictive drugs (*13*), which models human drug addiction (*14*). We applied this system to various transgenic mice to identify genes involved in the pathogenesis of drug addiction. Accordingly, we found that MHCI expressed in dopaminergic neurons plays a key role in decreased glutamatergic synaptic transmission and reward-seeking behavior. Moreover, repeated cocaine intake persistently reduced MHCI expression in dopaminergic neurons, and this deficiency contributed to the underlying mechanism of relapse to cocaine seeking.

RESULTS

Enhanced reward-seeking behavior in functional MHCI KO mice

We used our novel drug self-administration system on adult male wild-type (WT) and double-KO mice of β2M and TAP1 ($\beta2M^{-/-}TAP1^{-/-}$), both of which are necessary proteins for MHCI function (*1*), for analysis of cocaine (Coc) or vehicle (Veh) self-administration. Upon a nose-poke into the active hole (active nose-pokes), mice received an intrathecal cocaine infusion (Fig. 1A), paired with a brief tone and light illumination as the conditioned stimulus (Fig. 1B). This protocol enabled WT and $\beta2M^{-/-}TAP1^{-/-}$ mice to acquire similar cocaine self-administration behavior during the 10-day acquisition period (fig. S1A). After a 10-day extinction period, active nose-poke reinstatement in response to the conditioned stimulus without cocaine was used to measure relapse to cocaine-seeking behavior (*15*).

[1]Department of Psychology and Behavioral Neuroscience, Hamamatsu University School of Medicine, 1-20-1 Handayama, Higashi-ku, Hamamatsu 431-3192, Japan. [2]Department of Regenerative and Infectious Pathology, Hamamatsu University School of Medicine, 1-20-1 Handayama, Higashi-ku, Hamamatsu 431-3192, Japan. [3]Department of Liberal Arts, Faculty of Medicine, Saitama Medical University, 38 Morohongo, Moroyama-machi, Iruma-gun, Saitama 350-0495, Japan. [4]Department of Neurophysiology, Hamamatsu University School of Medicine, 1-20-1 Handayama, Higashi-ku, Hamamatsu 431-3192, Japan. [5]Department of Psychiatry, Hamamatsu University School of Medicine, 1-20-1 Handayama, Higashi-ku, Hamamatsu 431-3192, Japan.
*Corresponding author. Email: nakahara@hama-med.ac.jp (D.N.); murakami@saitama-med.ac.jp (G.M.)

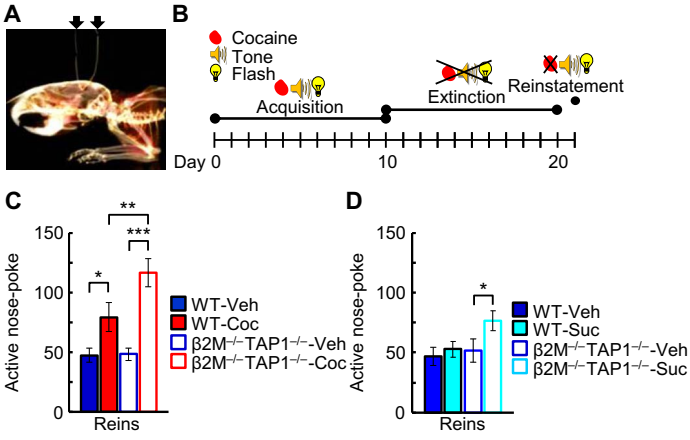

Fig. 1. Cocaine- and sucrose-seeking behavior in WT and functional MHCI knockout (KO) mice. (**A**) Computed tomography image showing a mouse with a microdialysis probe implanted into the supracerebellar cistern. Arrows indicate perfusion tubing. (**B**) Cocaine self-administration procedure. (**C**) Active nose-pokes in WT and β2M$^{-/-}$TAP1$^{-/-}$ mice that self-administered vehicle (Veh) or cocaine (Coc) during the reinstatement period [two-way analysis of variance (ANOVA); genotype: $F_{(1,77)} = 4.2$, $P < 0.05$; treatment: $F_{(1,77)} = 17.2$, $P < 0.001$; genotype × treatment: $F_{(1,77)} = 5.9$, $P < 0.05$; $n = 21$ for WT-Veh, $n = 19$ for WT-Coc, $n = 21$ for KO-Veh, and $n = 20$ for KO-Coc). (**D**) Active nose-pokes of WT and β2M$^{-/-}$TAP1$^{-/-}$ mice that self-administered Veh or sucrose (Suc) during the reinstatement period [two-way ANOVA; treatment: $F_{(1,27)} = 5.5$, $P < 0.05$; genotype × treatment: $F_{(1,27)} = 4.5$, $P < 0.05$; $n = 8$ for WT-Veh, $n = 8$ for WT-Suc, $n = 7$ for KO-Veh, and $n = 8$ for KO-Suc]. All data are represented as means ± SEM. *$P < 0.05$, **$P < 0.01$, and ***$P < 0.001$.

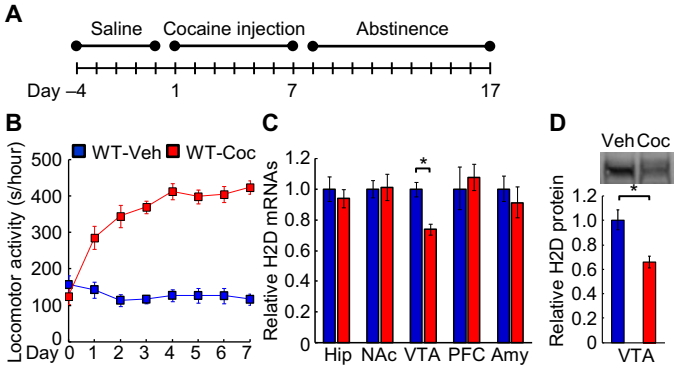

Fig. 2. Cocaine-induced decrease of MHCI expression in the VTA. (**A**) Experimenter-administered cocaine injection procedure. (**B**) Locomotor activity in WT mice injected with Veh or Coc. (**C**) H2D mRNA levels in the hippocampus (Hip), NAc, VTA, prefrontal cortex (PFC), and amygdala (Amy) of WT mice injected with Veh or Coc (Student's *t* test, $P < 0.05$; $n = 8$ for Veh and $n = 8$ for Coc). (**D**) H2D protein in the VTA of WT mice injected with Veh or Coc (Student's *t* test, $P < 0.05$; $n = 8$ for Veh and $n = 6$ for Coc). All data are represented as means ± SEM and labeled as in (B). *$P < 0.05$.

Although both genotypes displayed relapse, the degree of increased active nose-pokes induced by cocaine cues was higher in β2M$^{-/-}$TAP1$^{-/-}$ mice than WT mice (Fig. 1C). The groups exhibited no differences in nose-poke frequency into a dummy hole with no reinforcement (inactive nose-pokes), locomotor activity during this period, or active nose-pokes during other periods, suggesting that increased active nose-pokes are due to enhanced cocaine seeking rather than general hyperactivity (fig. S1, B to D). In contrast, cocaine-induced locomotor activity was enhanced in β2M$^{-/-}$TAP1$^{-/-}$ mice, particularly during the acquisition period (fig. S1D), indicating that MHCI also contributes to cocaine-induced behavioral sensitization. Consistent with this, β2M$^{-/-}$TAP1$^{-/-}$ mice showed greater behavioral sensitization after seven daily cocaine injections than WT mice, and this enhancement was significantly larger in β2M$^{-/-}$TAP1$^{-/-}$ mice than single-KO mice of β2M or TAP1 (fig. S1E).

Next, we analyzed the contribution of MHCI to reward-seeking behavior for a natural reward such as sucrose (fig. S2A). Although much larger increases in active nose-pokes were observed for sucrose than vehicle in both genotypes during the acquisition period, active nose-pokes during reinstatement were similar between sucrose and vehicle groups in WT mice (Fig. 1D and fig. S2B), showing transient reinforcement of sucrose, consistent with another report (*16*). In contrast, β2M$^{-/-}$TAP1$^{-/-}$ mice showed more active nose-pokes for sucrose than vehicle during the reinstatement period. However, because an ascending fixed-ratio (FR) schedule of reinforcement during the acquisition period amplifies cue-induced sucrose reinstatement, it is possible that increasing FR may augment sucrose reinstatement in WT mice in this experiment (*17*). The numbers of inactive nose-pokes and locomotor activity in all periods, active nose-pokes during other periods (fig. S2, B to D), and sucrose preference (fig. S2, E and F) were similar between genotypes. These results indicate that MHCI plays a crucial role in suppressing reward-seeking behavior, and its deficiency contributes to relapse to reward seeking for cocaine as well as a natural reward.

Cocaine-induced persistent reduction of MHCI in dopaminergic neurons

We found that MHCI, an immune protein, plays a key role in suppressing reward-seeking behavior. Given that previous studies have demonstrated cocaine-induced modulation of immune signaling (*18*), it is possible that cocaine intake may impair MHCI function, causing relapse to cocaine-seeking behavior. Therefore, we analyzed MHCI expression levels in brain regions associated with cocaine addiction in WT mice (*19*, *20*). First, we used an experimenter-administered cocaine injection procedure (Fig. 2A). Seven daily cocaine injections caused behavioral sensitization (Fig. 2B) that persisted for at least 10 days of abstinence (*21*). On the day after abstinence, mice were decapitated for mRNA analysis by quantitative real-time polymerase chain reaction (RT-PCR). In the brain regions examined, mRNA levels of H2D [a classical MHCI gene (*22*, *23*)] were specifically reduced in the VTA of cocaine-injected mice after abstinence (Fig. 2C). H2D protein levels were also decreased in VTA (Fig. 2D). Alternatively, cocaine-induced interferon-γ mRNA elevation in VTA returned to control levels during abstinence (fig. S3A), suggesting that persistent H2D mRNA reduction is unlikely due to a transient inflammatory response induced by cocaine injection.

Next, we analyzed H2D mRNA levels in VTA of WT mice used for behavioral analysis of cocaine self-administration on the day after reinstatement. Repeated cocaine intake led to decreased H2D and H2K [another classical MHCI gene (*8*, *22*)], concomitant with altered expression of MHCI-related genes (fig. S3B). Furthermore, we observed statistically significant negative correlation between H2D mRNA and the number of active nose-pokes divided by the number of inactive nose-pokes during the reinstatement period in WT mice ($R^2 = 0.26$, $P < 0.05$) (fig. S3C). Conversely, H2D reduction was not observed with the sucrose self-administration protocol (fig. S3E). Collectively, these findings indicate that cocaine persistently reduced MHCI expression in the VTA, which possibly contributed to relapse to cocaine-seeking behavior.

We also compared cocaine-induced increases in expression of dopamine transporter (DAT), tyrosine hydroxylase (TH), and dopamine

receptor D2, candidate molecular markers associated with cocaine addiction (*24*). Expression levels of DAT and TH were elevated in VTA with the experimenter-administered cocaine injection procedure (fig. S3A), whereas expression levels of all dopamine-related genes were considerably higher in $\beta2M^{-/-}TAP1^{-/-}$ mice with the cocaine self-administration model (fig. S3D). With sucrose self-administration, a similar but not significant pattern of dopamine-related gene expression was observed in $\beta2M^{-/-}TAP1^{-/-}$ mice (fig. S3E). These results suggest that enhanced dopamine-related gene expression is also caused by reduced MHCI expression.

Expression of MHCI in dopaminergic neurons

Because MHCI is expressed in the VTA and substantia nigra of the midbrain, with dopaminergic neurons present in both regions (*9*, *25*–*27*), we performed immunohistochemistry to determine the VTA cell types that express MHCI under normal conditions. First, we characterized the specificity of antibodies against H2D using a detergent-free method to stain only cell surface–expressed MHCI in VTA slices prepared from WT and $\beta2M^{-/-}TAP1^{-/-}$ mice (fig. S4A) (*8*). An antibody against H2D produced specific staining in WT but not $\beta2M^{-/-}TAP1^{-/-}$ mice (Fig. 3, A and B, and fig. S4B).

Analysis of cell types expressing H2D showed that soma-like staining of H2D predominantly colocalized with TH, a marker of dopaminergic neurons, suggesting that H2D/MHCI is expressed in dopaminergic neurons (Fig. 3C and fig. S4C). In contrast, staining of ionized calcium-binding adapter molecule 1, glial fibrillary acidic protein, and glutamic acid decarboxylase (GAD67), markers of microglia, glial cells, and GABAergic neurons, respectively, were predominantly observed in the substantia nigra reticulata and did not overlap with H2D (figs. S4D and S7). We next assessed subcellular localization of MHCI in VTA dopaminergic neurons because postsynaptic MHCI localization is reported in some brain regions (*8*, *28*–*30*). In addition to soma-like staining, higher-magnification images showed punctuate H2D/MHCI immunostaining that extensively overlapped with the postsynaptic marker postsynaptic density protein–95 (PSD-95) and not the presynaptic marker synaptophysin (Fig. 3, D and E). Together, these results demonstrate that H2D/MHCI is localized at postsynaptic dopaminergic neurons.

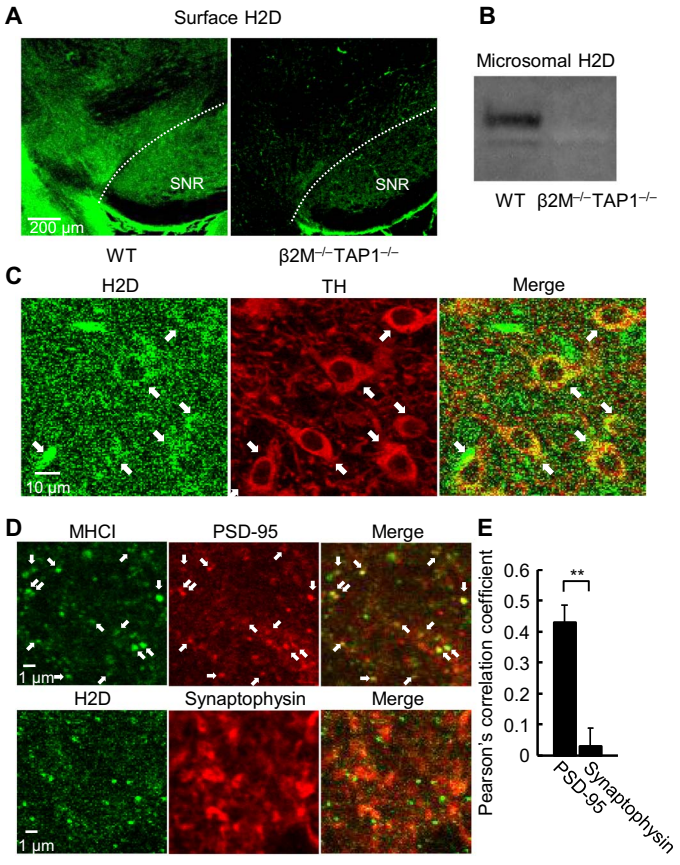

Fig. 3. Immunohistochemical analysis of MHCI localization in the VTA. (**A**) Immunohistochemistry with an antibody against H2D to detect cell surface–expressed protein in the VTA of WT and $\beta2M^{-/-}TAP1^{-/-}$ mice. SNR, substantia nigra reticulata. (**B**) Western blot analysis of H2D protein in microsomal fractions prepared from the whole brain of WT and $\beta2M^{-/-}TAP1^{-/-}$ mice. (**C**) Double staining of H2D and TH, a marker of dopaminergic neurons, in the VTA of WT mice. Arrows indicate colocalization between H2D and TH. (**D**) Double staining of MHCI/H2D with postsynaptic (PSD-95) and presynaptic (synaptophysin) markers in the VTA of WT mice. Arrows indicate colocalization between MHCI and PSD-95. (**E**) Pearson's correlation coefficient to quantify the degree of colocalization between MHCI and PSD-95 or synaptophysin. Costes' test showed statistically significant correlation between MHCI and PSD-95. Data are represented as means ± SEM. Student's *t* test, $^{**}P < 0.01$.

Enhanced cocaine-induced increase in glutamatergic synaptic transmission in dopaminergic neurons of functional MHCI KO mice

Given the role of MHCI in decreased glutamatergic synaptic transmission (*8*, *9*, *21*), persistent cocaine-induced reduction of MHCI expression at postsynaptic dopaminergic neurons may lead to long-lasting potentiation of glutamatergic synaptic inputs, a candidate mechanism for enduring cocaine-seeking behavior (*16*). Thus, we performed ex vivo whole-cell patch-clamp recordings in dopaminergic neurons of freshly prepared VTA slices from WT and $\beta2M^{-/-}TAP1^{-/-}$ mice after a 10-day extinction period in the cocaine self-administration experiment. Cocaine-induced modulation of spines was also compared between genotypes (*31*). First, we examined the ratio of α-amino-3-hydroxy-5-methyl-4-isoxazole propionic acid receptor (AMPAR)– to *N*-methyl-D-aspartate receptor (NMDAR)–mediated excitatory postsynaptic currents (EPSCs) in VTA dopaminergic neurons as a measure of the strength of glutamatergic synaptic transmission to these neurons (*32*). Similar magnitudes of cocaine-induced increases in the AMPAR/NMDAR ratio were observed in WT and $\beta2M^{-/-}TAP1^{-/-}$ mice (Fig. 4A). This increase was also observed after a 3-week extinction period in WT mice (fig. S5A). In contrast, $\beta2M^{-/-}TAP1^{-/-}$ mice showed a larger AMPAR/NMDAR ratio than WT mice after cocaine administration. Furthermore, AMPAR/NMDAR ratio 24 hours after a single experimenter injection of cocaine (20 mg/kg body weight) resulted in a similar AMPAR/NMDAR ratio between WT and $\beta2M^{-/-}TAP1^{-/-}$ mice (fig. S9). Overall, this indicates that cocaine-induced increase in AMPAR/NMDAR ratio is enhanced by repeated cocaine intake in combination with MHCI deficiency.

Alteration of AMPAR/NMDAR ratio can be attributed to modulation of AMPAR and/or NMDAR currents. In previous studies, NMDAR currents were larger in $\beta2M^{-/-}TAP1^{-/-}$ than WT mice (*10*, *33*). We also observed larger NMDAR currents in $\beta2M^{-/-}TAP1^{-/-}$ than WT mice after cocaine administration (fig. S5B). Because of these larger NMDAR currents in $\beta2M^{-/-}TAP1^{-/-}$ mice, the cocaine-induced increase in AMPAR/NMDAR ratio of similar magnitude across genotypes (Fig. 4A) suggests that the magnitude of AMPAR current increase is larger

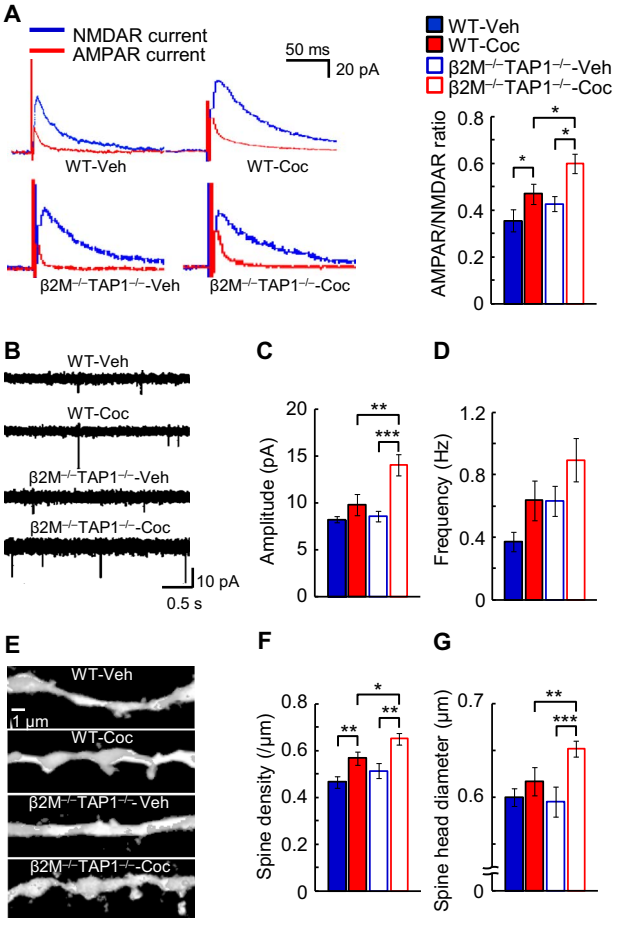

Fig. 4. Ex vivo whole-cell patch-clamp recordings and spine analysis in VTA dopaminergic neurons after an extinction period of cocaine self-administration. (**A**) AMPAR/NMDAR ratio in VTA dopaminergic neurons of WT and β2M$^{-/-}$TAP1$^{-/-}$ mice after an extinction period of Veh or Coc self-administration [two-way ANOVA; genotype: $F_{(1,42)} = 5.3$, $P < 0.05$; treatment: $F_{(1,42)} = 10.8$, $P < 0.01$; $n = 13$ slices for WT-Veh, $n = 14$ slices for WT-Coc, $n = 9$ slices for KO-Veh, and $n = 10$ slices for KO-Coc; VTA slices were prepared from six mice in each group]. (**B** to **D**) Representative traces (B), amplitude (C), and frequency (D) of mEPSCs in VTA dopaminergic neurons of WT and β2M$^{-/-}$TAP1$^{-/-}$ mice after an extinction period of Veh or Coc self-administration [two-way ANOVA; amplitude: treatment: $F_{(1,29)} = 10.8$, $P < 0.001$; genotype × treatment: $F_{(1,29)} = 5.1$, $P < 0.05$; frequency: genotype: $F_{(1,29)} = 4.6$, $P < 0.05$; treatment: $F_{(1,29)} = 6.6$, $P < 0.05$; $n = 8$ slices for WT-Veh, $n = 9$ slices for WT-Coc, $n = 8$ slices for KO-Veh, and $n = 8$ slices for KO-Coc; VTA slices were prepared from four mice in each group]. (**E** to **G**) Three-dimensional images of dendritic spines (E) and summary of spine density (F) and head diameter (G) in VTA dopaminergic neurons of WT and β2M$^{-/-}$TAP1$^{-/-}$ mice after an extinction period of Veh or Coc self-administration [two-way ANOVA: spine density: genotype: $F_{(1,80)} = 5.5$, $P < 0.05$; treatment: $F_{(1,80)} = 17.3$, $P < 0.001$; $n = 27$ slices for WT-Veh, $n = 18$ slices for WT-Coc, $n = 13$ slices for KO-Veh, and $n = 26$ slices for KO-Coc; diameter: treatment: $F_{(1,83)} = 12.7$, $P < 0.01$; genotype × treatment: $F_{(1,83)} = 3.9$, $P < 0.05$; $n = 27$ slices for WT-Veh, $n = 21$ slices for WT-Coc, $n = 13$ slices for KO-Veh, and $n = 26$ slices for KO-Coc; VTA slices were prepared from six mice in each group]. All data are represented as means ± SEM and labeled as in (A). *$P < 0.05$, **$P < 0.01$, and ***$P < 0.001$.

in β2M$^{-/-}$TAP1$^{-/-}$ mice. Corroboratively, compared with WT mice, β2M$^{-/-}$TAP1$^{-/-}$ mice exhibited a higher degree of cocaine-induced increases in AMPAR-mediated miniature EPSC (mEPSC) amplitude (Fig. 4, B and C, and fig. S5C) and spine head diameter (Fig. 4, E and G, and fig. S5E), both of which are associated with AMPAR expression levels (*34*). These interactive effects between MHCI and cocaine show that functional MHCI KO enhances cocaine-induced increases in AMPAR-mediated synaptic transmission to dopaminergic neurons, as observed in the nucleus accumbens (NAc) (*21*).

Conversely, WT and β2M$^{-/-}$TAP1$^{-/-}$ mice showed similar magnitudes of cocaine-induced increases in spine density, with higher values in β2M$^{-/-}$TAP1$^{-/-}$ than WT mice after cocaine administration (Fig. 4F). A similar but not significant pattern was also observed in mEPSC frequency (Fig. 4D and fig. S5D), showing a noninteractive effect between MHCI and cocaine, as observed for NMDA-induced currents (fig. S5B). Spine density is associated with mEPSC frequency and NMDAR expression levels (*34*); therefore, NMDAR-associated functions may mediate this noninteractive effect of MHCI with cocaine. Altogether, these results indicate that by enhancing AMPAR- and NMDAR-associated functions, the respective interactive and noninteractive effects of MHCI and cocaine lead to strongest glutamatergic synaptic transmission in VTA dopaminergic neurons from β2M$^{-/-}$TAP1$^{-/-}$ mice that have self-administered cocaine (fig. S5G).

Suppressed relapse to cocaine seeking by H2D overexpression in VTA dopaminergic neurons

To confirm that cocaine-induced reduction of MHCI expression in VTA dopaminergic neurons is necessary for relapse to cocaine seeking, we overexpressed H2D specifically in these neurons of WT mice using recombinant adeno-associated virus type 2 (rAAV-2) encoding H2D [or enhanced green fluorescent protein (EGFP) as a control] under control of the TH promoter (Fig. 5A) (*35*, *36*). rAAV-2 microinjection into VTA caused specific expression of these genes in VTA dopaminergic neurons (4.1 ± 1.3–fold for H2D), as observed by fluorescence immunohistochemistry (Fig. 5B and fig. S6A). Enhanced expression of H2D protein and mRNA were confirmed by immunoblotting and RT-PCR, respectively (Fig. 5, C and D). This was accompanied by a moderate increase in MHCI-related genes supporting H2D function without alteration of TH mRNA in VTA (fig. S6B).

Although WT mice expressing EGFP and overexpressing H2D showed similar acquisition of cocaine self-administration (fig. S6C), the number of active nose-pokes during the reinstatement period was reduced to almost half in H2D-overexpressing mice compared with EGFP-expressing mice (Fig. 5E). Moreover, there were no differences in active nose-pokes during other periods or inactive nose-pokes and locomotor activity during all periods (fig. S6, D to F), suggesting that reduced active nose-pokes in H2D-overexpressing mice during the reinstatement period is due to suppressed cocaine seeking rather than nonspecific changes in motor activity. Thus, persistent cocaine-induced reduction of MHCI in VTA dopaminergic neurons is necessary for relapse to cocaine seeking.

DISCUSSION

In summary, functional MHCI KO in mice promoted relapse to cocaine seeking and also showed enduring reward seeking for a natural reward, which was not observed in WT mice. In contrast, H2D overexpression in dopaminergic neurons suppressed the relapse to cocaine seeking. Dopaminergic neuronal activity is a primary reward signal in the brain (*37*), which is regulated by glutamatergic synaptic input (*16*). MHCI is necessary for decreased glutamatergic synaptic transmission (*8*, *9*); therefore, our findings suggest that postsynaptic MHCI expressed at dopaminergic neurons is critical for decreased glutamatergic synaptic

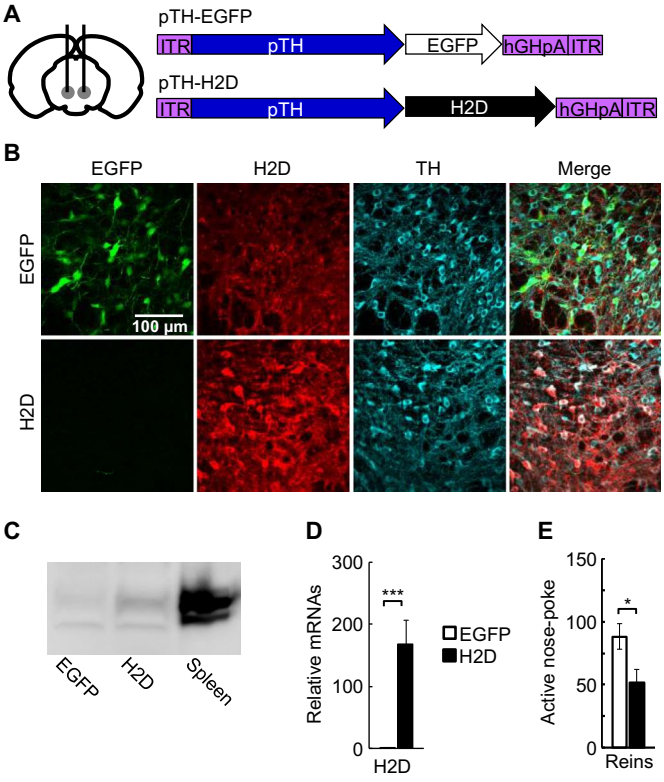

Fig. 5. Cocaine-seeking behavior in WT mice overexpressing H2D in VTA dopaminergic neurons. (**A**) Recombinant AAV-2 constructs encoding EGFP and H2D under control of the TH promoter (pTH). ITR, inverted terminal repeat; hGHpA, human growth hormone polyA sequence. (**B**) Immunostaining of EGFP, H2D, and TH in the VTA of mice expressing EGFP (upper) or H2D (lower). TH expression was identified in >90% of neurons expressing these genes. (**C**) Protein levels of H2D in the VTA of EGFP- or H2D-expressing mice. (**D**) mRNA levels of H2D in VTA of EGFP- and H2D-expressing mice (Student's *t* test, $P < 0.001$; $n = 7$ for EGFP and $n = 8$ for H2D). (**E**) Active nose-pokes of EGFP- and H2D-expressing mice during reinstatement of cocaine self-administration (Student's *t* test, $P < 0.05$; $n = 8$ for EGFP and $n = 8$ for H2D). All data are represented as means ± SEM and labeled as in (D). *$P < 0.05$ and ***$P < 0.001$.

input and suppressed relapse to cocaine seeking. Because MHCI consists of multiple genes with compensatory functions (*8*, *22*, *23*), we used global KO β2M and TAP1 mice for functional MHCI KO. Although H2D overexpression, predominantly in dopaminergic neurons, suppressed the relapse to cocaine seeking, it is important to confirm that MHCI (particularly in dopaminergic neurons) contributes to the relapse to cocaine seeking using conditional KO mice. Furthermore, repeated cocaine intake persistently reduced MHCI expression, which was accompanied by increased glutamatergic synaptic transmission to VTA dopaminergic neurons, and ultimately, enduring cocaine-seeking behavior. Altogether, these results suggest that cocaine-induced reduction of MHCI expression in VTA dopaminergic neurons may be an underlying mechanism for relapse to cocaine seeking.

In our previous study, we developed intrathecal drug administration as an alternative to intravenous administration to allow 24-hour unlimited access to cocaine in mice (*2*). We rigorously investigated cocaine self-administration behavior and observed similar behaviors with intrathecal and intravenous self-administration methods, except for the appearance of escalation and binge patterns. However, it is important to compare the molecular effects of cocaine between these methods in future studies because there may be differences due to the different administration routes.

Among the brain regions examined, repeated cocaine intake persistently reduced MHCI expression only in the VTA (Fig. 2C). This suggests that MHCI plays a key role in reinstatement of cocaine-seeking behavior particularly in this region. The VTA is an important region for cue-induced (*38*) and drug-induced (*39*, *40*) reinstatement, as well as the initiation phase of cocaine self-administration (*41*). Here, we also show that H2D overexpression specifically in VTA dopaminergic neurons attenuates cue-induced reinstatement. In contrast, cocaine-induced locomotor activity did not recover in mice overexpressing H2D in VTA dopaminergic neurons (fig. S6, F to H), although it was enhanced in $\beta2M^{-/-}TAP1^{-/-}$ mice lacking MHCI function throughout the brain (fig. S1D). These findings imply that MHCI expressed in other brain regions, such as the NAc, contributes to cocaine-induced behavioral sensitization (*21*).

Regarding the relapse mechanism for cocaine seeking, a persistent increase in glutamatergic synaptic transmission to VTA dopaminergic neurons has been suggested (*16*, *32*). This persistent increase may be attributable to enhanced potentiation and suppressed depression of glutamatergic synaptic transmission to dopaminergic neurons. Accordingly, increased expression of genes for synaptic potentiation (for example, brain-derived neurotrophic factor) was identified after repeated intake of addictive drugs (*42*–*45*). However, contribution of genes for synaptic depression to drug addiction has not yet been demonstrated. Here, we show that MHCI plays a key role in synaptic depression, with cocaine intake causing persistent reduction of MHCI expression in VTA dopaminergic neurons. These results support our idea that repeated cocaine intake induces persistently reduced MHCI expression and leads to enduring enhancement of synaptic transmission in VTA dopaminergic neurons, overall resulting in long-lasting cocaine-seeking behavior.

Accompanied by increased glutamatergic synaptic transmission, repeated cocaine intake also up-regulated dopamine-related gene expression. Because dopamine-related gene expression is regulated by neuronal activity (*46*), this observed up-regulation may be attributable to increased synaptic transmission induced by suppressed MHCI expression. A tendency of MHCI reduction was detected before abstinence from cocaine intake, although up-regulation of dopamine-related gene expression was observed after abstinence (fig. S3A). Hence, persistent cocaine-induced reduction of MHCI expression may increase glutamatergic synaptic transmission, which possibly up-regulates dopamine-related gene expression in VTA dopaminergic neurons.

Cocaine also has non-neuronal actions at immunocompetent cells in the central nervous system. Activation of central immune signaling pathways is considered to play a significant role in cocaine addiction via modulation of neuronal-glial interactions, although this effect is complementary and these pathways alone do not produce relevant addictive phenotypes (*18*). It should be noted that immune activation generally induces MHCI expression, whereas cocaine intake suppresses MHCI expression in dopaminergic neurons despite activation of immune signaling pathways. Thus, the effect of cocaine is complex, contributing to the activation of central immune signaling pathways and decreased MHCI expression, both of which may lead to the establishment of neural circuits underlying cocaine addiction. The detailed relationship between these two effects of cocaine on immune signaling factors should be investigated in future studies, although significant contribution of immune signaling factors to cocaine addiction can be expected.

Although our study focused on a role of MHCI in adults, MHCI is highly expressed in the developing brain (*2*, *47*) and contributes to neural circuit organization. Deficiency of MHCI function leads to abnormal neural circuits such as strengthened projections from the retina to lateral geniculate nucleus (*9*), increased glutamatergic synaptic transmission to cortical and hippocampal neurons (*8*, *28*), and lack of left-right synapses and circuit asymmetry via NMDAR regulation (*48*). Given that dopaminergic neurons are implicated not only in drug addiction but also in neurodevelopmental disorders, MHCI in dopaminergic neurons may be involved in these disorders. Recent clinical studies have revealed strong association between the *MHC* locus and schizophrenia (*49*, *50*) and autism (*51*). Consequently, our finding that MHCI plays a critical role in decreased glutamatergic synaptic transmission to dopaminergic neurons and reward-seeking behavior potentially provides a novel landmark in the pathogenesis of drug addiction as well as insight into the molecular basis of neurodevelopmental disorders.

MATERIALS AND METHODS

Study design

The present study was designed to determine whether MHCI plays a role in relapse to cocaine seeking. For this purpose, double-KO mice for the genes β2M and TAP1 ($\beta2M^{-/-}TAP1^{-/-}$), which are both necessary for MHCI function, were compared to WT mice in terms of behavioral, molecular biological, electrophysiological, and biochemical end points after cocaine or vehicle administration. No statistical methods were used to predetermine sample size, but the sample sizes used are similar to those reported in the literature. Mice were not excluded from the study except those that died before and during analysis. The present data show that MHCI plays a critical role in suppression of relapse to reward seeking and is potentially a novel landmark in the pathogenesis of drug addiction.

Reagents and animal models

Double-KO ($\beta2M^{-/-}TAP1^{-/-}$) and WT F1 mice were generated from C57BL/6 $\beta2M^{-/-}$ and $TAP1^{-/-}$ single-KO mice, which were purchased from the Jackson Laboratory. To prevent substrain divergence, we obtained the F2–4 male offspring of $\beta2M^{-/-}TAP1^{-/-}$ and WT mice by breeding homozygous mice. Mice between 8 and 10 weeks were used for experiments. Mice were screened by PCR-based analysis of tail genomic DNA to identify WT and β2M and TAP1 homozygous mutant or heterozygous mutant animals. There were no obvious phenotypic abnormalities in the VTA of $\beta2M^{-/-}TAP1^{-/-}$ mice (fig. S7). All mice were individually housed under a 12-hour light/12-hour dark cycle (lights on at 7:00 and lights off at 19:00) in a temperature-controlled environment (23° to 25°C) with food and water available ad libitum in a specific pathogen–free environment (*52*). Cocaine hydrochloride (Dai-Nihon) was dissolved in Ringer's solution [138 mM NaCl, 2.4 mM KCl, and 1.2 mM $CaCl_2$ (pH 7.0)] for cocaine self-administration or saline (0.9% NaCl) for experimenter-administered injection. Solutions were filter-sterilized before use. All procedures were approved by the University Committee on the Use and Care of Experimental Animals at the Hamamatsu University School of Medicine. All efforts were made to minimize the number of animals used and their suffering.

Cocaine self-administration procedure

See the Supplementary Materials for the surgery method and chamber for cocaine self-administration. Daily 24-hour sessions of cocaine self-administration were conducted without any initial priming under unlimited drug-access conditions. Mice were first subjected to a cocaine acquisition period, where a nose-poke into the active hole (active nose-poke) led to a single cocaine infusion under an FR for one schedule of reinforcement for 5 days (Fig. 1B). This was followed by an FR2 schedule for 5 days, during which two active nose-pokes were required for cocaine infusion. Each response was reinforced by 12 μg of cocaine infusion over 30 s through the dialysis membrane. We had previously confirmed that this dose is suitable for unlimited cocaine self-administration sessions (*13*). As conditioned stimuli, an active nose-poke was accompanied by a brief tone, with each cocaine infusion signaled by illumination of a light above the hole that remained on for 60 s, during which nose-pokes were still counted but no cocaine infused. Nose-pokes in the inactive hole (inactive nose-pokes) were also recorded but had no consequences. In $\beta2M^{-/-}TAP1^{-/-}$ and WT mice, the number of active nose-pokes for cocaine but not vehicle almost doubled when the schedule was changed from FR1 to FR2, confirming similar motivation for cocaine self-administration (fig. S1A). In the following 10-day extinction period, neither cocaine nor conditioned stimuli resulted from active nose-pokes. This extinction period was followed by a reinstatement period where conditioned stimuli without cocaine infusion were activated by active nose-pokes. On the last day of each period, behaviors were analyzed against data during the 12-hour dark phase. In this analysis, no criteria were implemented for exclusion of mice that did not show addictive phenotypes. When criteria were similarly implemented in our previous work (*53*) (at least 10 reinforcers per day, with a minimum of 70% responding on the active hole and <20% variability in the number of reinforced responses for 3 days on the FR2 schedule), 11 WT- and 5 $\beta2M^{-/-}TAP1^{-/-}$-cocaine treated mice were excluded. Almost the same result was observed, with a slight increase in active nose-pokes, for cocaine during reinstatement in both WT and $\beta2M^{-/-}TAP1^{-/-}$ mice (from 79 to 81 in WT-Coc, from 116 to 124 in $\beta2M^{-/-}TAP1^{-/-}$-Coc).

Experimenter-administration procedure

After acclimation to the testing chamber and saline injections over 4 days, WT mice were intraperitoneally injected daily with vehicle (0.9% NaCl) or cocaine hydrochloride (20 mg/kg body weight) during the light phase for seven consecutive days (Fig. 2A). For motor activity tests, vehicle or cocaine was intraperitoneally injected at 10 ml/kg body weight, and locomotor activity was measured over 60 min. During the following 10 days of abstinence, all mice were individually housed in the colony room.

Sucrose self-administration procedure

Sucrose self-administration was conducted in the same operant chamber but with addition of a spout above the active nose-poke hole for oral delivery of sucrose solution (fig. S2A). The sucrose self-administration procedure was nearly identical to the cocaine self-administration protocol except that the acquisition period consisted of a 10-day FR1 schedule because of the relatively slow acquisition of sucrose self-administration. Mice received a 50-μl volume of 10% sucrose solution delivered over 1 min upon one active nose-poke. Nose-pokes were allowed for the first 2 hours of the dark phase for each day of the acquisition and extinction periods, and for all 12 hours of the dark phase during reinstatement. All mice were food-restricted to 85 to 90% of their body weight during all periods. See the Supplementary Materials for the sucrose preference test.

Quantitative RT-PCR analysis

RNA was prepared from isolated brain regions, as described previously (*54*). Briefly, after behavioral studies, mice were deeply anesthetized and decapitated. Brains were quickly removed and stored at −80°C. Coronal brain slices (1 mm in thickness) were prepared from the entire brain using a mouse brain matrix, with specific brain regions isolated using razor blades. Total RNA was isolated from each region using TRI Reagent according to the manufacturer's instructions (Funakoshi). Complementary DNA (cDNA) was reverse-transcribed from the total RNA using a High-Capacity cDNA Archive Kit (Applied Biosystems) according to the manufacturer's instructions. Quantitative RT-PCR was performed using the StepOne Real-Time PCR System (Applied Biosystems). All primers used in this experiment are described in the Supplementary Materials.

Western blotting

Mice were deeply anesthetized, and whole brains were removed and quickly frozen at −80°C. Coronal brain slices (1 mm in thickness) were prepared for the entire brain using a mouse brain matrix, and the VTA was isolated using razor blades. Western blotting was performed as described before, but with a slight modification (*55*). Protein was detected with a primary antibody against H2D (28-14-8, diluted 1:500; Thermo Fisher Scientific). Immunolabeling was analyzed using a LAS3000 Image Analyzer (Fujifilm).

Immunohistochemistry

Immunohistochemistry was performed as described before, but with a slight modification (*55*). Briefly, mice were deeply anesthetized and transcardially perfused with 4% paraformaldehyde for 5 min. Whole brains were removed, and slices were prepared on a cryostat (HM550, Thermo Fisher Scientific). Brain slices were incubated for 2 hours at room temperature in blocking buffer containing phosphate-buffered saline (PBS), 5% normal goat serum (Wako), 10% bovine serum albumin (BSA) (Sigma-Aldrich), and 0.5% Triton X-100. Next, slices were incubated at 4°C overnight with primary antibodies in staining buffer (3% BSA and 0.5% Triton X-100 in PBS). For double staining, brain slices were sequentially incubated with individual primary antibodies. Images were captured by confocal microscopy (FV1000-D; Olympus). For higher-magnification images (Fig. 3D), a high digital zoom (×2.0) with 100× objective lens was used, which allowed resolution of pre- and postsynapses. All antibodies and their dilutions are described in the Supplementary Materials.

Cell surfaces expressing MHCI and H2D were immunostained using a detergent-free method (*8*) without Triton X-100 (Fig. 3A and fig. S4B). Brains were weakly perfusion-fixed with 4% paraformaldehyde at 2.0 ml/min, with freshly prepared slices used for staining because strong fixation interferes with MHCI-antibody binding (*25*). GAD67-GFP knock-in mice were immunostained with anti-GFP antibody for identification of GABAergic neurons (fig. S4D) (*56*).

Whole-cell patch-clamp recordings

Whole-cell patch-clamp recordings were performed as described previously, but with some modifications (*57*). Briefly, 250-μm horizontal slices including the VTA were prepared from mice the day after the end of the cocaine self-administered extinction period. Mice were deeply anesthetized and transcardially perfused with 25 ml of ice-cold sucrose solution containing 220.0 mM sucrose, 2.5 mM KCl, 1.25 mM NaH_2PO_4, 10.0 mM $MgSO_4$, 0.5 mM $CaCl_2$, 26.0 mM $NaHCO_3$, 30.0 mM glucose, 3.0 mM pyruvate-Na, and 1.0 mM ascorbic acid–Na. Brains were rapidly removed and submerged in cold oxygenated sucrose solution for 1 min. After removing the forebrain, cerebellum, and top of the brain with razor blades, slices were cut into sucrose solution using a linear slicer (PRO 7, Dosaka) with a ceramic blade (7550/1/C, Campden Instruments Limited). Slices were placed in an interface storage chamber (BSC3; Scientific Systems Design Inc.) containing standard artificial cerebrospinal fluid (ACSF) consisting of 125 mM NaCl, 2.5 mM KCl, 1.25 mM NaH_2PO_4, 1.0 mM $MgSO_4$, 2.0 mM $CaCl_2$, 26.0 mM $NaHCO_3$, 1.0 mM ascorbic acid–Na, and 20.0 mM glucose, aerated with 95% O_2 and 5% CO_2 at 33°C for 2 hours. Slices were kept at room temperature until recordings.

Patch electrodes were fabricated from 1.5-mm diameter borosilicate capillary tubing (GD-1.5; Narishige) using a P97 horizontal puller (Sutter Instruments). Electrode resistance ranged from 3 to 6 megohms when filled with solution containing 117 mM cesium methanesulfonic acid, 20 mM Hepes, 0.4 mM EGTA, 2.8 mM NaCl, 5.0 mM TEA-Cl, 2.5 mM MgATP, and 0.25 mM NaGTP. The pH was adjusted to 7.2 with CsOH. For spine analysis, the pipette solution also included 0.2% biocytin. Individual slices were transferred to a recording chamber, perfused at 2 ml/min with aerated standard ACSF containing 100 μM picrotoxin, and maintained at 32°C. Dopaminergic neurons in the medial terminal nucleus of the VTA were identified in current clamps by the presence of large hyperpolarization-activated currents (Ih) during hyperpolarizing pulses from −70 mV (fig. S8). A tungsten bipolar electrode was placed approximately 100 μm rostral to the recording site, and EPSCs were evoked by 300-μs subthreshold stimuli at 0.1 Hz. Neurons were held at −70 or 40 mV as indicated for recordings. Recorded currents were filtered at 2 kHz and digitized at 1 to 10 kHz using DigiData1322A and pCLAMP9 software (Molecular Devices).

For analysis of AMPAR/NMDAR ratio, dopaminergic neurons were voltage-clamped at +40 mV. After observing stable EPSCs for several minutes, EPSCs were recorded in the absence and presence of 50 μM D(−)-2-amino-5-phosphonopentanoic acid (AP5) to measure total and AMPAR currents, respectively. For analysis, 10 to 20 EPSCs were averaged for each recording. NMDAR currents were calculated by subtracting the AMPAR current from total current. AMPAR/NMDAR ratio was estimated by dividing peak AMPAR-mediated EPSC by peak NMDAR-mediated EPSC. It should be noted that the effect of functional MHCI KO on AMPAR/NMDAR ratio was observed after daily cocaine self-administration for 10 days (Fig. 4A), but not 24 hours after single experimenter injection (20 mg/kg body weight) (fig. S9). NMDA-induced currents were recorded by perfusing 50 μM NMDA for 10 min at +40 mV. For mEPSC analysis, neurons were held at −70 mV in the presence of 50 μM AP5 and 0.5 μM tetrodotoxin, and spontaneous activity was recorded for 20 min. Detection criteria were set at >7 pA. Data were analyzed using Clampfit 9 (Molecular Devices).

Spine analysis

After electrophysiological recordings, slices were fixed in 4% paraformaldehyde at 4°C overnight. Biocytin was detected with Alexa Fluor 488 conjugated to streptavidin (1:500; Molecular Probes). Imaging was performed as described before, but with a slight modification (*55*). Briefly, sequential *z*-series scans were acquired using a confocal microscope (FV1000-D, Olympus) at high zoom (×2.0) with a 100× oil immersion lens. For analysis of spine morphology, three-dimensional information was acquired every 0.5 μm from approximately 10 sequential *z*-series sections. In each slice, two to three secondary dendrites (80 μm in length on average) were analyzed. Spine density, spine head diameter, and spine neck length were analyzed using Neurolucida (MBF Bioscience).

There was no effect of genotype or treatment (cocaine/vehicle self-administration) on neck length (fig. S5F).

Microinjection of rAAV-2 in VTA

See the Supplementary Materials for construction of rAAV-2 expressing EGFP or H2D. WT mice were deeply anesthetized and placed in a stereotaxic instrument (Narishige). A hole was made on each side of the skull with a dental drill, and a Hamilton microsyringe with 32-gauge needle (Hamilton) was vertically inserted into the VTA (2.7 mm posterior, 0.5 mm lateral, and 4.0 mm ventral to bregma). A 0.2-μl volume of rAAV-2 (titer, 6.0×10^{11}) encoding H2D or EGFP under control of the TH promoter was microinjected into each side for 5 min. The needle was kept in place for an additional 5 min before it was slowly withdrawn. Microinjections were followed by surgery for self-administration. Mice were individually housed in the colony room and allowed to recover for 14 days, during which the dialysis probe was flushed daily with Ringer's solution to maintain patency. After cocaine self-administration experiments, brains were removed and sliced to verify the needle location (fig. S10). H2D or EGFP expression levels were confirmed in these slices. Staining was performed as described in the section on immunohistochemistry, except for slice preparation. Briefly, the forebrain, cerebellum, and top of the brain were removed with razor blades, and 200-μm coronal slices were cut into PBS using a vibratome (DTK1500, Dosaka).

Statistical analysis

All data are presented as means ± SEM. Group means of WT and $\beta2M^{-/-}TAP1^{-/-}$ mice administered cocaine or vehicle were compared using two-way ANOVA (genotype × treatment) followed by least significant difference post hoc analysis. mRNA levels before and after abstinence (fig. S3A) were compared using one-way ANOVA followed by Bonferroni post hoc analysis. Paired *t* tests were used to compare cocaine versus vehicle and EGFP versus H2D expression groups.

SUPPLEMENTARY MATERIALS

Supplementary material for this article is available at http://advances.sciencemag.org/cgi/content/full/4/3/eaap7388/DC1

Supplementary Materials and Methods

fig. S1. Cocaine-seeking behavior in WT and $\beta2M^{-/-}TAP1^{-/-}$ mice.

fig. S2. Behavioral analysis of WT and $\beta2M^{-/-}TAP1^{-/-}$ mice in sucrose self-administration and sucrose preference.

fig. S3. mRNA analysis of dopamine-related genes and MHCI-related genes in the VTA.

fig. S4. MHCI immunostaining in the VTA.

fig. S5. Extended electrophysiological analysis.

fig. S6. Analysis of mice overexpressing H2D in VTA dopaminergic neurons.

fig. S7. Comparison of VTA cellular organization between WT and $\beta2M^{-/-}TAP1^{-/-}$ mice.

fig. S8. Identification of dopaminergic neurons in whole-cell patch-clamp recordings.

fig. S9. AMPAR/NMDAR ratio after single cocaine injection.

fig. S10. Histological verification of inserted needle placement after behavioral analysis of H2D- and EGFP-expressing mice.

References (*58*–*60*)

REFERENCES AND NOTES

1. H. G. Ljunggren, L. Van Kaer, M. S. Sabatine, H. Auchincloss Jr., S. Tonegawa, H. L. Ploegh, MHC class I expression and CD8+ T cell development in TAP1/beta 2-microglobulin double mutant mice. *Int. Immunol.* **7**, 975–984 (1995).
2. R. A. Corriveau, G. S. Huh, C. J. Shatz, Regulation of class I MHC gene expression in the developing and mature CNS by neural activity. *Neuron* **21**, 505–520 (1998).
3. T. J. Dixon-Salazar, L. Fourgeaud, C. M. Tyler, J. R. Poole, J. J. Park, L. M. Boulanger, MHC class I limits hippocampal synapse density by inhibiting neuronal insulin receptor signaling. *J. Neurosci.* **34**, 11844–11856 (2014).
4. B. M. Elmer, M. L. Estes, S. L. Barrow, A. K. McAllister, MHCI requires MEF2 transcription factors to negatively regulate synapse density during development and in disease. *J. Neurosci.* **33**, 13791–13804 (2013).
5. T. Kim, G. S. Vidal, M. Djurisic, C. M. William, M. E. Birnbaum, K. C. Garcia, B. T. Hyman, C. J. Shatz, Human LilrB2 is a β-amyloid receptor and its murine homolog PirB regulates synaptic plasticity in an Alzheimer's model. *Science* **341**, 1399–1404 (2013).
6. M. Djurisic, G. S. Vidal, M. Mann, A. Aharon, T. Kim, A. Ferrao Santos, Y. Zuo, M. Hübener, C. J. Shatz, PirB regulates a structural substrate for cortical plasticity. *Proc. Natl. Acad. Sci. U.S.A.* **110**, 20771–20776 (2013).
7. J. Syken, T. Grandpre, P. O. Kanold, C. J. Shatz, PirB restricts ocular-dominance plasticity in visual cortex. *Science* **313**, 1795–1800 (2006).
8. M. W. Glynn, B. M. Elmer, P. A. Garay, X.-B. Liu, L. A. Needleman, F. El-Sabeawy, A. K. McAllister, MHCI negatively regulates synapse density during the establishment of cortical connections. *Nat. Neurosci.* **14**, 442–451 (2011).
9. G. S. Huh, L. M. Boulanger, H. Du, P. A. Riquelme, T. M. Brotz, C. J. Shatz, Functional requirement for class I MHC in CNS development and plasticity. *Science* **290**, 2155–2159 (2000).
10. P. A. Nelson, J. R. Sage, S. C. Wood, C. M. Davenport, S. G. Anagnostaras, L. M. Boulanger, MHC class I immune proteins are critical for hippocampus-dependent memory and gate NMDAR-dependent hippocampal long-term depression. *Learn. Mem.* **20**, 505–517 (2013).
11. G. F. Koob, M. Le Moal, Drug abuse: Hedonic homeostatic dysregulation. *Science* **278**, 52–58 (1997).
12. D. Nakahara, M. Nakamura, M. Iigo, H. Okamura, Bimodal circadian secretion of melatonin from the pineal gland in a living CBA mouse. *Proc. Natl. Acad. Sci. U.S.A.* **100**, 9584–9589 (2003).
13. M. Nakamura, S. Gao, H. Okamura, D. Nakahara, Intrathecal cocaine delivery enables long-access self-administration with binge-like behavior in mice. *Psychopharmacology (Berl)* **213**, 119–129 (2011).
14. L. A. Knackstedt, P. W. Kalivas, Extended access to cocaine self-administration enhances drug-primed reinstatement but not behavioral sensitization. *J. Pharmacol. Exp. Ther.* **322**, 1103–1109 (2007).
15. V. Deroche-Gamonet, D. Belin, P. V. Piazza, Evidence for addiction-like behavior in the rat. *Science* **305**, 1014–1017 (2004).
16. B. T. Chen, M. S. Bowers, M. Martin, F. W. Hopf, A. M. Guillory, R. M. Carelli, J. K. Chou, A. Bonci, Cocaine but not natural reward self-administration nor passive cocaine infusion produces persistent LTP in the VTA. *Neuron* **59**, 288–297 (2008).
17. A.-C. Bobadilla, C. Garcia-Keller, J. A. Heinsbroek, M. D. Scofield, V. Chareunsouk, C. Monforton, P. W. Kalivas, Accumbens mechanisms for cued sucrose seeking. *Neuropsychopharmacology* **42**, 2377–2386 (2017).
18. J. K. Coller, M. R. Hutchinson, Implications of central immune signaling caused by drugs of abuse: Mechanisms, mediators and new therapeutic approaches for prediction and treatment of drug dependence. *Pharmacol. Ther.* **134**, 219–245 (2012).
19. P. W. Kalivas, K. McFarland, Brain circuitry and the reinstatement of cocaine-seeking behavior. *Psychopharmacology (Berl)* **168**, 44–56 (2003).
20. G. F. Koob, N. D. Volkow, Neurocircuitry of addiction. *Neuropsychopharmacology* **35**, 217–238 (2009).
21. M. Edamura, G. Murakami, H. Meng, M. Itakura, R. Shigemoto, A. Fukuda, D. Nakahara, Functional deficiency of MHC class I enhances LTP and abolishes LTD in the nucleus accumbens of mice. *PLOS ONE* **9**, e107099 (2014).
22. A. Datwani, M. J. McConnell, P. O. Kanold, K. D. Micheva, B. Busse, M. Shamloo, S. J. Smith, C. J. Shatz, Classical MHCI molecules regulate retinogeniculate refinement and limit ocular dominance plasticity. *Neuron* **64**, 463–470 (2009).
23. H. Lee, B. K. Brott, L. A. Kirkby, J. D. Adelson, S. Cheng, M. B. Feller, A. Datwani, C. J. Shatz, Synapse elimination and learning rules co-regulated by MHC class I H2-D^b. *Nature* **509**, 195–200 (2014).
24. S. L. Vrana, K. E. Vrana, T. R. Koves, J. E. Smith, S. I. Dworkin, Chronic cocaine administration increases CNS tyrosine hydroxylase enzyme activity and mRNA levels and tryptophan hydroxylase enzyme activity levels. *J. Neurochem.* **61**, 2262–2268 (1993).
25. Z. C. Peng, K. Kristensson, M. Bentivoglio, Distribution and temporal regulation of the immune response in the rat brain to intracerebroventricular injection of interferon-gamma. *Exp. Neurol.* **154**, 403–417 (1998).
26. C. Cebrián, F. A. Zucca, P. Mauri, J. A. Steinbeck, L. Studer, C. R. Scherzer, E. Kanter, S. Budhu, J. Mandelbaum, J. P. Vonsattel, L. Zecca, J. D. Loike, D. Sulzer, MHC-I expression renders catecholaminergic neurons susceptible to T-cell-mediated degeneration. *Nat. Commun.* **5**, 3633 (2014).
27. H. Lindå, H. Hammarberg, F. Piehl, M. Khademi, T. Olsson, Expression of MHC class I heavy chain and beta2-microglobulin in rat brainstem motoneurons and nigral dopaminergic neurons. *J. Neuroimmunol.* **101**, 76–86 (1999).
28. C. A. Goddard, D. A. Butts, C. J. Shatz, Regulation of CNS synapses by neuronal MHC class I. *Proc. Natl. Acad. Sci. U.S.A.* **104**, 6828–6833 (2007).
29. L. A. Needleman, X.-B. Liu, F. El-Sabeawy, E. G. Jones, A. K. McAllister, MHC class I molecules are present both pre- and postsynaptically in the visual cortex during

postnatal development and in adulthood. *Proc. Natl. Acad. Sci. U.S.A.* **107**, 16999–17004 (2010).
30. S. Thams, P. Brodin, S. Plantman, R. Saxelin, K. Karre, S. Cullheim, Classical major histocompatibility complex class I molecules in motoneurons: New actors at the neuromuscular junction. *J. Neurosci.* **29**, 13503–13515 (2009).
31. F. Sarti, S. L. Borgland, V. N. Kharazia, A. Bonci, Acute cocaine exposure alters spine density and long-term potentiation in the ventral tegmental area. *Eur. J. Neurosci.* **26**, 749–756 (2007).
32. M. A. Ungless, J. L. Whistler, R. C. Malenka, A. Bonci, Single cocaine exposure in vivo induces long-term potentiation in dopamine neurons. *Nature* **411**, 583–587 (2001).
33. L. Fourgeaud, C. M. Davenport, C. M. Tyler, T. T. Cheng, M. B. Spencer, L. M. Boulanger, MHC class I modulates NMDA receptor function and AMPA receptor trafficking. *Proc. Natl. Acad. Sci. U.S.A.* **107**, 22278–22283 (2010).
34. J. Noguchi, A. Nagaoka, S. Watanabe, G. C. R. Ellis-Davies, K. Kitamura, M. Kano, M. Matsuzaki, H. Kasai, In vivo two-photon uncaging of glutamate revealing the structure-function relationships of dendritic spines in the neocortex of adult mice. *J. Physiol.* **589**, 2447–2457 (2011).
35. J. Liu, J. P. Merlie, R. D. Todd, K. L. O'Malley, Identification of cell type-specific promoter elements associated with the rat tyrosine hydroxylase gene using transgenic founder analysis. *Mol. Brain Res.* **50**, 33–42 (1997).
36. M. S. Oh, S. J. Hong, Y. Huh, K.-S. Kim, Expression of transgenes in midbrain dopamine neurons using the tyrosine hydroxylase promoter. *Gene Ther.* **16**, 437–440 (2008).
37. W. A. Carlezon Jr., M. J. Thomas, Biological substrates of reward and aversion: A nucleus accumbens activity hypothesis. *Neuropharmacology* **56** (suppl. 1), 122–132 (2009).
38. P. E. M. Phillips, G. D. Stuber, M. L. A. V. Heien, R. M. Wightman, R. M. Carelli, Subsecond dopamine release promotes cocaine seeking. *Nature* **422**, 614–618 (2003).
39. W. Sun, C. K. Akins, A. E. Mattingly, G. V. Rebec, Ionotropic glutamate receptors in the ventral tegmental area regulate cocaine-seeking behavior in rats. *Neuropsychopharmacology* **30**, 2073–2081 (2005).
40. H. D. Schmidt, K. R. Famous, R. C. Pierce, The limbic circuitry underlying cocaine seeking encompasses the PPTg/LDT. *Eur. J. Neurosci.* **30**, 1358–1369 (2009).
41. J. D. Steketee, P. W. Kalivas, Drug wanting: Behavioral sensitization and relapse to drug-seeking behavior. *Pharmacol. Rev.* **63**, 348–365 (2011).
42. J. W. Grimm, L. Lu, T. Hayashi, B. T. Hope, T.-P. Su, Y. Shaham, Time-dependent increases in brain-derived neurotrophic factor protein levels within the mesolimbic dopamine system after withdrawal from cocaine: Implications for incubation of cocaine craving. *J. Neurosci.* **23**, 742–747 (2003).
43. L. Lu, J. Dempsey, S. Y. Liu, J. M. Bossert, Y. Shaham, A single infusion of brain-derived neurotrophic factor into the ventral tegmental area induces long-lasting potentiation of cocaine seeking after withdrawal. *J. Neurosci.* **24**, 1604–1611 (2004).
44. L. Pu, Q.-s. Liu, M.-m. Poo, BDNF-dependent synaptic sensitization in midbrain dopamine neurons after cocaine withdrawal. *Nat. Neurosci.* **9**, 605–607 (2006).
45. H. D. Schmidt, G. R. Sangrey, S. B. Darnell, R. L. Schassburger, J.-H. J. Cha, R. C. Pierce, G. Sadri-Vakili, Increased brain-derived neurotrophic factor (BDNF) expression in the ventral tegmental area during cocaine abstinence is associated with increased histone acetylation at BDNF exon I-containing promoters. *J. Neurochem.* **120**, 202–209 (2012).
46. T. D. Aumann, K. Egan, J. Lim, W. C. Boon, C. R. Bye, H. K. Chua, N. Baban, C. L. Parish, L. Bobrovskaya, P. Dickson, M. K. Horne, Neuronal activity regulates expression of tyrosine hydroxylase in adult mouse substantia nigra pars compacta neurons. *J. Neurochem.* **116**, 646–658 (2011).
47. M. A. Chacon, L. M. Boulanger, MHC class I protein is expressed by neurons and neural progenitors in mid-gestation mouse brain. *Mol. Cell. Neurosci.* **52**, 117–127 (2013).
48. A. Kawahara, S. Kurauchi, Y. Fukata, J. Martínez-Hernández, T. Yagihashi, Y. Itadani, R. Sho, T. Kajiyama, N. Shinzato, K. Narusuye, M. Fukata, R. Luján, R. Shigemoto, I. Ito, Neuronal major histocompatibility complex class I molecules are implicated in the generation of asymmetries in hippocampal circuitry. *J. Physiol.* **591**, 4777–4791 (2013).
49. J. Shi, D. F. Levinson, J. Duan, A. R. Sanders, Y. Zheng, I. Pe'er, F. Dudbridge, P. A. Holmans, A. S. Whittemore, B. J. Mowry, A. Olincy, F. Amin, C. R. Cloninger, J. M. Silverman, N. G. Buccola, W. F. Byerley, D. W. Black, R. R. Crowe, J. R. Oksenberg, D. B. Mirel, K. S. Kendler, R. Freedman, P. V. Gejman, Common variants on chromosome 6p22.1 are associated with schizophrenia. *Nature* **460**, 753–757 (2009).
50. H. Stefansson, R. A. Ophoff, S. Steinberg, O. A. Andreassen, S. Cichon, D. Rujescu, T. Werge, O. P. H. Pietiläinen, O. Mors, P. B. Mortensen, E. Sigurdsson, O. Gustafsson, M. Nyegaard, A. Tuulio-Henriksson, A. Ingason, T. Hansen, J. Suvisaari, J. Lonnqvist, T. Paunio, A. D. Børglum, A. Hartmann, A. Fink-Jensen, M. Nordentoft, D. Hougaard, B. Norgaard-Pedersen, Y. Böttcher, J. Olesen, R. Breuer, H.-J. Möller, I. Giegling, H. B. Rasmussen, S. Timm, M. Mattheisen, I. Bitter, J. M. Réthelyi, B. B. Magnusdottir, T. Sigmundsson, P. Olason, G. Masson, J. R. Gulcher, M. Haraldsson, R. Fossdal, T. E. Thorgeirsson, U. Thorsteinsdottir, M. Ruggeri, S. Tosato, B. Franke, E. Strengman, L. A. Kiemeney; Genetic Risk and Outcome in Psychosis (GROUP), I. Melle, S. Djurovic, L. Abramova, V. Kaleda, J. Sanjuan, R. de Frutos, E. Bramon, E. Vassos, G. Fraser, U. Ettinger, M. Picchioni, N. Walker, T. Toulopoulou, A. C. Need, D. Ge, J. Lim Yoon, K. V. Shianna, N. B. Freimer, R. M. Cantor, R. Murray, A. Kong, V. Golimbet, A. Carracedo, C. Arango, J. Costas, E. G. Jönsson, L. Terenius, I. Agartz, H. Petursson, M. M. Nöthen, M. Rietschel, P. M. Matthews, P. Muglia, L. Peltonen, D. St Clair, D. B. Goldstein, K. Stefansson, D. A. Collier, Common variants conferring risk of schizophrenia. *Nature* **460**, 744–747 (2009).
51. L. A. Needleman, A. K. McAllister, The major histocompatibility complex and autism spectrum disorder. *Dev. Neurobiol.* **72**, 1288–1301 (2012).
52. S. Takabayashi, T. Nishikawa, H. Katoh, A novel *Kit* gene mutation in CF1 mice involved in the extracellular domain of the KIT protein. *Exp. Anim.* **61**, 435–444 (2012).
53. M. Nakamura, S. Gao, H. Okamura, D. Nakahara, Intrathecal cocaine delivery enables long-access self-administration with binge-like behavior in mice. *Psychopharmacology (Berl)* **213**, 119–129 (2010).
54. G. Murakami, R. G. Hunter, C. Fontaine, A. Ribeiro, D. Pfaff, Relationships among estrogen receptor, oxytocin and vasopressin gene expression and social interaction in male mice. *Eur. J. Neurosci.* **34**, 469–477 (2011).
55. G. Murakami, Y. Hojo, M. Ogiue-Ikeda, H. Mukai, P. Chambon, K. Nakajima, Y. Ooishi, T. Kimoto, S. Kawato, Estrogen receptor KO mice study on rapid modulation of spines and long-term depression in the hippocampus. *Brain Res.* **1621**, 133–146 (2014).
56. T. Furukawa, J. Yamada, T. Akita, Y. Matsushima, Y. Yanagawa, A. Fukuda, Roles of taurine-mediated tonic $GABA_A$ receptor activation in the radial migration of neurons in the fetal mouse cerebral cortex. *Front. Cell. Neurosci.* **8**, 88 (2014).
57. K. Egawa, K. Kitagawa, K. Inoue, M. Takayama, C. Takayama, S. Saitoh, T. Kishino, M. Kitagawa, A. Fukuda, Decreased tonic inhibition in cerebellar granule cells causes motor dysfunction in a mouse model of Angelman syndrome. *Sci. Transl. Med.* **4**, 163ra157 (2012).
58. K. B. J. Franklin, G. Paxinos, in *Paxinos and Franklin's the mouse brain in stereotaxic coordinates* (Academic Press, 2012), vol. 1.
59. J. L. Merritt, T. Nguyen, J. Daniels, D. Matern, D. B. Schowalter, Biochemical correction of very long–chain Acyl-CoA dehydrogenase deficiency following adeno-associated virus gene therapy. *Mol. Ther.* **17**, 425–429 (2009).
60. L. M. Boulanger, C. J. Shatz, Immune signalling in neural development, synaptic plasticity and disease. *Nat. Rev. Neurosci.* **5**, 521–531 (2004).

Acknowledgments: We are grateful to A. Nozue, M. Kawashima, H.-R. Meng, M. Nakamura, S. Takabayashi, and Y. Koide for technical and experimental assistance; T. Hiranita, S. Toda, H. Ichinose, and T. Nagata for valuable discussions; and M. Murakami for discussion and comments on the manuscript. We thank R. James from Edanz Group (www.edanzediting.com/ac), for editing a draft of the manuscript. **Funding:** This study was supported by the Grants-in-Aid for Scientific Research (grant nos. JP2389076, JP25860392, JP15K19164, and JP17K08960) from the Japan Society for the Promotion of Science (to G.M.); the Grants-in-Aid for Scientific Research on Innovative Areas (grant no. 15H05872) from the Ministry of Education, Culture, Sports, Science (to A.F.), and Hamamatsu University School of Medicine project research. **Author contributions:** G.M. designed and performed all experiments, analyzed data, and wrote the manuscript. D.N. designed all experiments and reviewed all data and the manuscript. M.E. assisted in cocaine self-administration experiments. T.F. assisted in whole-cell patch-clamp recordings. A.F. reviewed results for whole-cell patch-clamp recordings and the manuscript. T.I. reviewed the manuscript. I.K. and H.K. assisted in construction of rAAV-2. **Competing interests:** The authors declare that they have no competing interests. **Data and materials availability:** All data needed to evaluate the conclusions in the paper are presented in the paper and/or the Supplementary Materials. Additional data related to this paper may be requested from the authors.

Submitted 22 August 2017
Accepted 7 February 2018
Published 14 March 2018
10.1126/sciadv.aap7388

Citation: G. Murakami, M. Edamura, T. Furukawa, H. Kawasaki, I. Kosugi, A. Fukuda, T. Iwashita, D. Nakahara, MHC class I in dopaminergic neurons suppresses relapse to reward seeking. *Sci. Adv.* **4**, eaap7388 (2018).

MHC class I in dopaminergic neurons suppresses relapse to reward seeking

Gen Murakami, Mitsuhiro Edamura, Tomonori Furukawa, Hideya Kawasaki, Isao Kosugi, Atsuo Fukuda, Toshihide Iwashita and Daiichiro Nakahara

Sci Adv **4** (3), eaap7388.
DOI: 10.1126/sciadv.aap7388